

Alterations of Choline Phospholipid Metabolism in Ovarian Tumor Progression: a NMR study

Alessandro Ricci , Egidio Iorio e Franca Podo.

Department of Cell Biology and Neurosciences, Section of Molecular and Cellular Imaging, Istituto Superiore di Sanità, Roma

Key words: **ovarian cancer; choline phospholipid metabolism; NMR; choline kinase; phosphocholine; phospholipase.**

INTRODUCTION

Epithelial ovarian cancer (EOC) is the leading cause of death in women with gynecological malignancies. Despite a relatively low incidence, EOC presents a high case-fatality ratio and the overall 5-year survival is still less than 45% (1). Women with organ-confined tumors have an excellent prognosis, but the majority of early stage cancers are asymptomatic or present non-specific and variable clinical manifestations, frequently delaying disease diagnosis. Indeed, over two-thirds of patients are diagnosed with advanced disease (FIGO stage III and IV) (2,3). Primary cytoreductive surgery followed by platinum-based chemotherapy is the standard treatment for this cancer. After a first high response rate, the patient usually relapses and the tumor becomes resistant to chemotherapy. Because EOC is intrapelvic, invasive methods are often unavoidable to monitor disease recurrence. Thus, there is a need for improved imaging methods to diagnose EOC and to monitor treatment response or tumor recurrence non-invasively.

The detection by nuclear magnetic resonance (NMR) of abnormal levels of choline phospholipid metabolites in tumor cells and tissues (reviewed in 4-7) has recently led to pilot studies aimed at evaluating the clinical utility of *in vivo*-localized NMR spectroscopy (MRS) and radiolabeled choline-based positron emission tomography (PET) in human cancers such as gliomas, breast, prostate and gynecologic carcinomas (8-9). However, clinical application of imaging methods based on detection of choline metabolites awaits further elucidation of the relationships between specific biochemical features and tumor progression *in vitro* and *in vivo*.

High-resolution NMR methods provide powerful means to fill this basic knowledge gap, by measuring steady-state levels and fluxes of metabolites in the pathways responsible for biosynthesis and catabolism of phosphatidylcholine (PC), the major phospholipid of eukaryotic cell membranes (Fig. 1). Substantially modified ¹H MRS spectral profiles have, in fact, been reported in the 3.20-3.24 ppm region (typical of trimethylammonium headgroups of PC precursors and catabolites, such as phosphocholine (PCho), glycerophosphocholine (GPC) and free choline (Cho)) upon malignant transformation of human mammary (10,11) and prostate epithelial cells (12). In particular, increases in the levels of PCho and total choline-containing (water-soluble) metabolites (tCho) have been reported in tumor cells, together with decreases in the GPC/PCho ratio (a phenomenon known as the "GPC-to-PCho switch" (6,10)).

To date, choline phospholipid metabolism in ovarian cancer has received only limited attention, despite preliminary indications of increased tCho in human ovary tumors and biopsies (13) and accumulation of PCho in ovarian carcinoma cell lines (14). In the present study, we quantified the intracellular levels of PC metabolites in the progression from non-tumoral ovarian surface epithelial (OSE) cells or immortalized cell variants to ovarian cancer cell lines and related these levels to quantitative differences in the basal activity of enzymes involved in PC biosynthesis and/or catabolism (see Fig. 1). In particular, the choline kinase (chok) basal activity rate and the overall PC-specific phospholipases C and D (PC-plc and PC-pld) activity were evaluated.

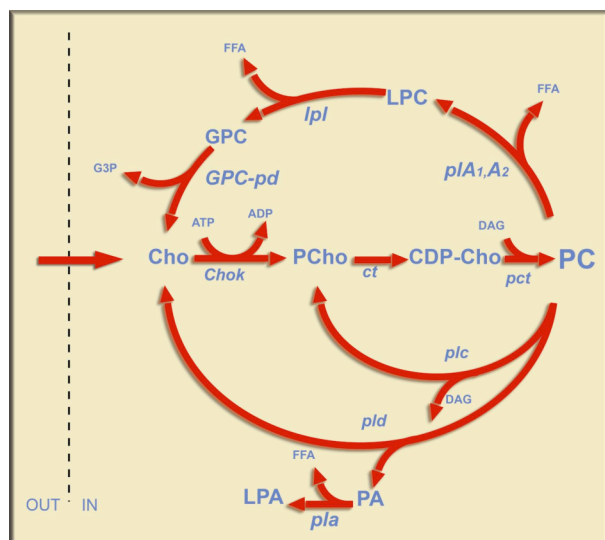


Figure 1. Schematic representation of phosphatidylcholine (PC) *de novo* biosynthesis and catabolism. *Metabolites*: CDP-Cho, cytidine diphosphate choline; Cho, choline; DAG, diacylglycerol; FFA, free fatty acid; G3P, *sn*-glycerol-3-phosphate; GPC glycerophosphocholine; PA, phosphatidate; PCho, phosphocholine. *Enzymes*: *chok*, choline kinase (EC 2.7.1.32); *ct*, cytidyltransferase (EC 2.7.7.15); *lpl*, lysophospholipase (EC 3.1.1.5); *pct* phosphocholine transferase (EC 2.7.8.2); *pd*, glycerophosphocholine phosphodiesterase (EC 3.1.4.2); *pla*, phospholipase A₂ (EC 3.1.1.4) and phospholipase A₁ (EC 3.1.1.32); *plc*, phospholipase C (EC 3.1.4.3); *pld*, phospholipase D (EC 3.1.4.4).

MATERIALS AND METHODS

Epithelial ovarian non-tumoral (EONT) and carcinoma cells. OSE cells were scraped from the surface of normal human ovaries obtained at surgery for benign or malignant gynecological diseases other than ovarian carcinoma. All human materials were obtained at the foundation of the Istituto Tumori di Milano with informed consent from patients. OSE cells were maintained in culture for 3-5 passages. Lifespan of short-term cultures of OSE cells was increased up to 15-16 passages by simian virus 40 (SV40) large T antigen transfection, thus obtaining IOSE cells. Stably immortalized IOSE cells were obtained by transfection with the cDNA of the catalytic subunit of the human telomerase reverse transcriptase (kindly provided by Dr. R. A. Weinberg, Whitehead Institute, Cambridge, MA), thus obtaining hTERT cells. Both IOSE and hTERT cells were maintained in the same medium as OSE cells. The following human serous ovarian carcinoma cell lines were used: IGROV1, a gift from J. Bénard, Institute Gustave Roussy, Villejuif, France; OVCAR3 and SKOV3 obtained from the American Type Culture Collection (ATCC); OVCA432, kindly provided by R. Knapp, Dana Farber Institute, Boston, MA; and CABA1 kindly provided by Dr. V. Dolo, University of L'Aquila, Italy (14). All EOC lines were of ascitic origin, except IGROV1 which derived from primary adenocarcinoma.

NMR spectroscopy. High-resolution NMR experiments (25°C) were performed at either 400 or 700 MHz (Bruker AVANCE spectrometers, Karlsruhe, Germany). ¹H NMR spectra of cell extracts were obtained using acquisition pulses, water pre-saturation, data processing and data analysis as already described (14). Quantification of individual metabolites was obtained from peak areas using correction factors determined by experiments at the equilibrium of magnetization (90° pulses, 30.00 s interpulse delay). In some samples parallel ³¹P NMR experiments were also performed at 161.97 MHz as previously described (15), in order to verify by an independent method PCho and GPC contents from peak areas of the respective signals at 3.78 and 0.49 ppm. The values of absolute metabolite concentrations obtained by the two methods were fully consistent and pooled together. Metabolite quantification was expressed as nmoles and normalized to the number of extracted cells (and also converted into fmol/μm³ cell volume, for comparison with other cell systems).

NMR assays on activity of basal chok, phospholipases and phosphodiesterases. We developed novel quantitative ¹H NMR assays, by simultaneously measuring precursor and product concentrations in lysates exposed to the appropriate substrates and cofactors (16). Assays on phospholipase-mediate PC hydrolysis were carried out by measuring choline formation upon addition of a monomeric short chain PC or exogenous GPC to lysates. Substrate and product

concentrations were simultaneously measured from the ^1H NMR peak areas (corrected for the respective factors of partial saturation of the magnetization vector).

Statistical analysis. Data were analyzed using GraphPad Software version 3.03. Statistical significance of differences was determined by one-way ANOVA or by Student's *t*-test, as specified. Differences were considered significant at $P < 0.05$.

RESULTS

Abnormal concentrations of PC metabolites are detected in ovarian cancer cells. One-dimensional ^1H NMR spectra of aqueous extracts revealed a more intense tCho resonance in five EOC cell lines (OVCAR3, CABA 1, IGROV1, SKOV3, OVCA432) as compared to normal (OSE) or immortalized (IOSE, hTERT) cells (example in Fig. 2). Moreover, analysis of expanded tCho spectral profiles showed that the relative areas of signal components due to individual PC metabolites (GPC, PCho and Cho) changed in the progression from non-tumor to carcinoma cells, PCho becoming predominant in all carcinoma cells tested (Fig. 2). High-resolution NMR revealed no significant differences between extracts of normal (OSE) and immortalized (IOSE and hTERT) cells in the absolute concentrations of individual PC metabolites or in the GPC/PCho ratio; thus, the respective concentrations of individual PC metabolites and the GPC/PCho ratios determined in eight independent experiments on epithelial ovarian non-tumoral (EONT, normal and immortalized) cells were averaged (mean \pm SD), with the following results : [GPC] = 1.9 ± 1.4 nmol/ 10^6 cells; [PCho] = 2.3 ± 0.9 nmol/ 10^6 cells; [Cho] = 1.1 ± 1.1 nmol/ 10^6 cells; GPC/PCho = 0.95 ± 0.93 and [tCho] = [GPC+PCho+Cho] = 5.2 ± 2.4 nmol/ 10^6 cells. The quite large scatter of some determinations could be attributed to the possible combination of several factors, including biological variability of cell cultures of OSE and their immortalized cell variants (derived from different individuals and analysed at different passages), variability in the timing of cell harvest and (to a lower extent) spectral deconvolution of overlapping peaks. In spite of data scatter, comparison of the average PCho contents in EONT cells with those in EOC cells (Fig. 2) revealed a 3- to 8-fold increase in the average content of this metabolite in all EOC cells ($P < 0.0001$). No significant differences ($P > 0.05$) were found between the levels of PC metabolites in individual EOC cell lines (all possessing highly malignant phenotypes).

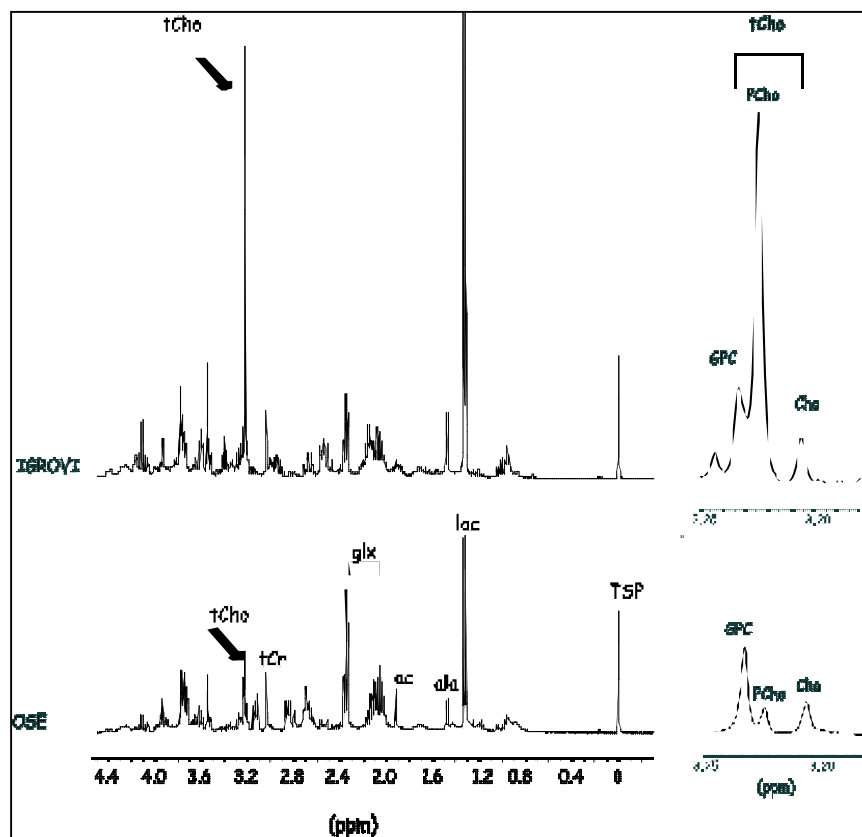


Fig. 2: Representative ^1H NMR spectra of aqueous extracts of ovary epithelial non-tumor (down) and tumor cells (up). Spectra (400 MHz) of normal OSE (1st-2nd passage), and IGROV1 ovarian carcinoma cells. Arrows indicate the resonance band of trimethylammonium moieties of “total choline-containing” metabolites (tCho, 3.20-3.24 ppm).

Consistent with the elevation in PCho content, the average pool size of tCho also increased (2.0- to 4.4-fold) in all EOC cells ($P < 0.0001$), while the average GPC/PCho ratio declined to values between 0.01 and 0.12 ($P < 0.01$). The latter finding is in general agreement with the “GPC-to-PCho switch” described for other types of cancer or oncogene-transformed cells (6, 10).

To further evaluate the role of [PCho] and GPC/PCho ratio in discriminating the biochemical behavior of EOC from EONT cells, two-dimensional maps were constructed by plotting either the PCho/tCho or the GPC/tCho ratio versus [tCho] for all sets of experimental data (Fig. 3). These analyses allowed clearcut separation of EOC from EONT cells into independent clusters ($P < 0.0001$ on both axes). In fact, EONT data were confined within areas characterized by an upper [tCho] value of $7.00 \text{ nmol}/10^6$ cells, an upper PCho/tCho value of 0.65, and a lower GPC/tCho value of 0.25 (95% confidence limits). The corresponding parameters measured for EOC cells were outside these thresholds (indicated by dashed lines in Fig. 3), with tCho contents extending from 7.4 to $32.5 \text{ nmol}/10^6$ cells, the PCho/tCho ratio ranging between 0.68 and 0.98, and the GPC/tCho ratio between 0.20 and less than 0.01.

The observed modifications in the levels of intracellular PC metabolites in EOC with respect to EONT cells could not be simply attributed to different cell doubling time, which was $41 \pm 8 \text{ h}$ for all cell systems analyzed, with the exception of OSE cells, which had an estimated doubling time of about 5 days. Nevertheless, this difference did not lead to any separation of OSE cell data outside the clusters typical of EONT cells (Fig. 3).

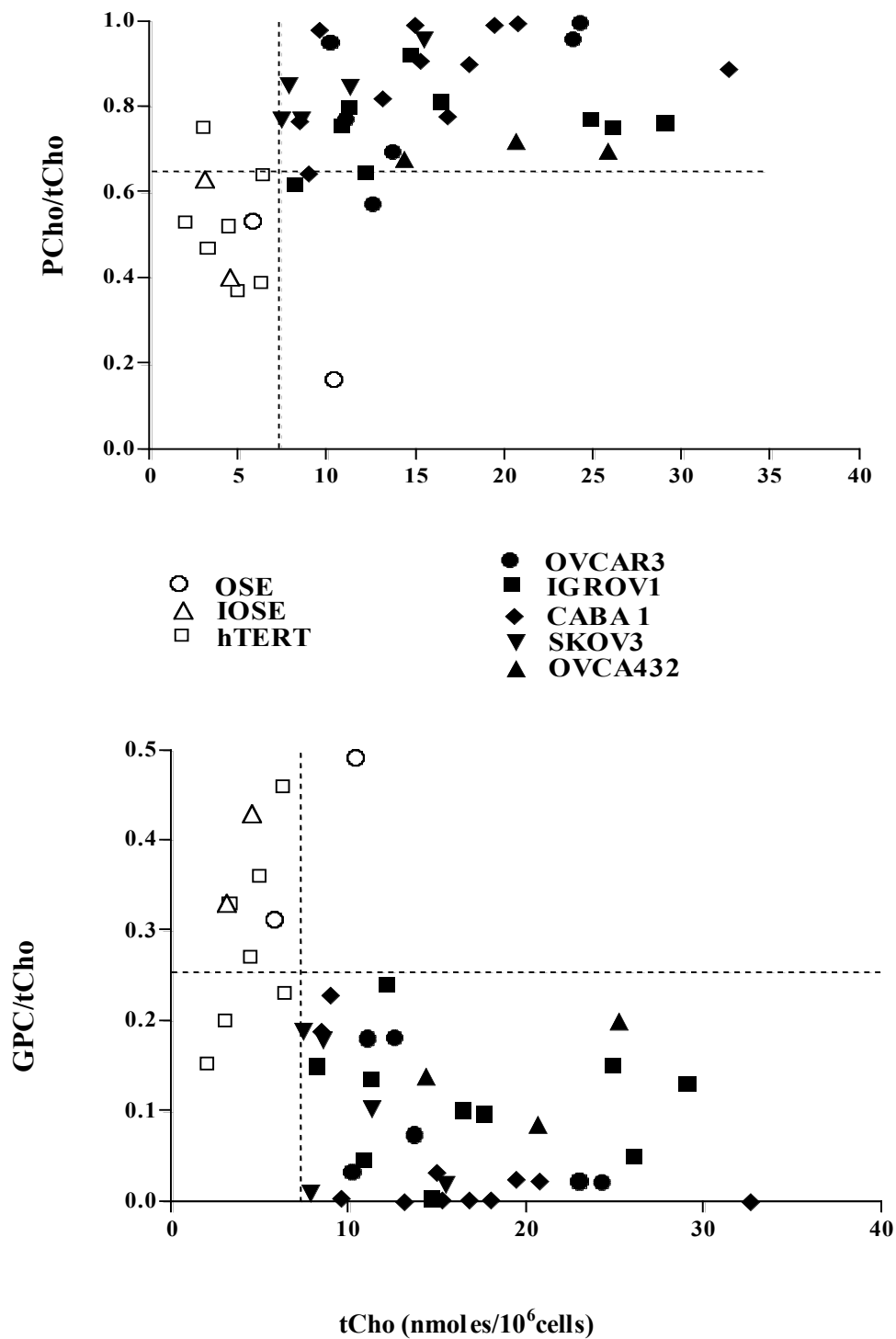


Figure 3. Clustering of EOC (● OVCAR3; ■ IGROV1; ◆ CABA 1; ▼ SKOV3; ▲ OVCA432) and EONT (○ OSE; △ IOSE; □ hTERT) cells' data in separate areas of two-dimensional $\{\text{PCho}/t\text{Cho}, [t\text{Cho}]\}$ and $\{\text{GPC}/t\text{Cho}, [t\text{Cho}]\}$ metabolic maps. Dashed lines represent the borders of EONT clustering areas constructed using the upper 95% confidence limit for $[t\text{Cho}]$, the upper 95% confidence limit for $\text{PCho}/t\text{Cho}$ and the lower 95% confidence limit for $\text{GPC}/t\text{Cho}$ values.

Enzymes responsible for PCho production are activated in ovarian cancer cells. Major contributions to PCho accumulation may derive from alternative or combined activation of enzymes involved in PC biosynthesis and/or catabolism (see Fig. 1), notably chok (responsible for Cho phosphorylation in the Kennedy pathway), PC-plc (responsible for PC hydrolysis into PCho and diacylglycerol) and pld (whose product, Cho, may in turn be converted into PCho by chok). Thus, enzymatic assays were performed to assess whether and to what extent these enzymes were activated in carcinoma cells.

The activity rate of chok was measured by NMR assay in cytosolic cell preparations of four EOC cell lines. Independent series of ^1H NMR experiments were carried out to determine the basal chok activity in hTERT cells. In view of the much higher levels of PCho formed during the reaction in EOC cell lysates, the kinetics of Cho phosphorylation could also be effectively monitored in these samples by ^{31}P NMR spectroscopy (two independent experiments on OVCAR3 and one for each of the other cell lines). ^1H and ^{31}P NMR gave consistent results. As reported in Fig. 4, these assays revealed an average basal chok rate of 0.5 ± 0.1 nmol/ 10^6 cells/h in hTERT cells, and a significant increase to 12-19-fold higher values in the overall set of investigated EOC cells ($P = 0.027$).

A number of enzymes responsible for metabolic fluxes in catabolic pathways of PC (PC-plc, pld and GPC-pd) also revealed a substantial activation in EOC as compared to EONT cells (Fig. 5).

Together, the results of all performed enzymatic assays indicated that activation of enzymes involved in both the biosynthetic and the catabolic pathways of the PC-cycle can contribute to the increased PCho levels measured in EOC as compared to EONT cells.

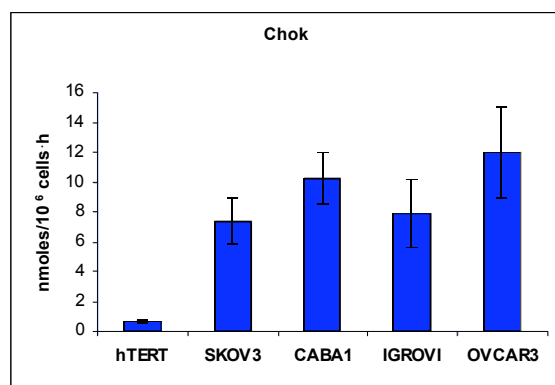


Fig.4 Basal activity rate of choline kinase (chok) in all EOC cells with respect to EONT cells. ($P=0.02$)

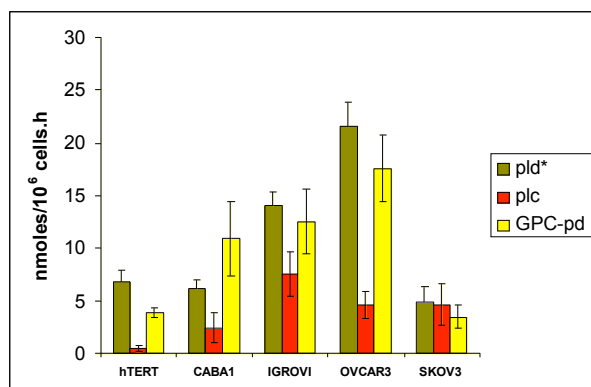


Fig. 5 Basal activity rates of PC-phospholipase D (pld), phospholipase C (plc) and glycerophosphocholine-phosphodiesterase (GPC-pd) all EOC cells lines compared to non-tumoral hTERT cells.

DISCUSSION AND PERSPECTIVES

Abnormal PC metabolism is reported as a common feature in breast and prostate cancer cell lines, with consequent alterations in the levels of NMR-detectable compounds such as PCho and tCho, and in the GPC/PCho ratio (4-7). In those experimental models, spectral changes did not correlate with cell doubling times; thus, these signals were proposed as fingerprints of tumor progression and/or endpoints of therapeutic treatment (7, 10, 11).

We demonstrate here that the quantitative alterations in intracellular levels of PCho, as well as the activation of both biosynthetic (chok) and catabolic (PC-plc and PC-pld) enzymes involved in intracellular PCho production, occur during ovary cancer progression. Intracellular concentrations of PCho in EOC cells reached average values of 7.5 – 17.3 nmol/10⁶ cells. These levels were 3-8 fold higher in EOC relative to EONT cells. Moreover, PCho represented the major fraction (over 70%) of the tCho resonance of EOC cells and thus accounted mainly for the increase in [tCho] and decrease in the GPC/PCho ratio occurring in tumor versus non-tumor cells.

These biochemical modifications did not correlate with the cell doubling time of ovarian carcinoma cells, arguing against the role of such changes as simple indicators of enhanced cancer cell proliferation. This body of evidence supports the general hypothesis that the multiple genetic changes occurring during carcinogenesis, and the associated alterations in growth factor-mediated cell signaling pathways, may ultimately result in induction or downregulation of enzymes involved in the PC-cycle (see Fig. 1).

These aspects appear particularly interesting in view of current efforts in molecular therapeutics and pharmacogenomics aimed at identifying new targets which may be relatively specific for growth, progression and survival of ovarian cancer (17).

Besides addressing new questions on the relationships between PC cycle and signal transduction pathways, the observed increase in chok in EOC cells may provide further support to the use of ¹¹C- or ¹⁸F-choline as radiotracers in PET examinations of primary pelvic tumors and lymph-node metastases (8, 9) as an alternative to ¹⁸F-fluorodeoxyglucose (FDG), whose abundant radioactivity excretion into the bladder may hamper image interpretation (18, 19). Finally, the *in vitro* NMR spectral and biochemical patterns detected in the present study have qualitative similarities with those in breast cancer cells. Thus, the high-resolution and *in vivo* MRS methods already successfully applied to mammary carcinoma patients (20) may well prove useful in ovary cancer patients. In particular, the here reported quantification of PC metabolites in cultured EOC cell lines may provide the grounds for interpreting MRS measurements on the “choline” signal *in vivo*, in terms of tumour progression, relapse or response to therapy.

The overall body of presented data may help elucidate aspects of EOC biology and provide a rational basis for further developing clinical non-invasive imaging methods suitable for ovary cancer diagnosis and follow-up.

ACKNOWLEDGEMENT

This work is carried out in collaboration with Dr. S. Canevari and Dr. D. Mezzananza, Istituto Nazionale Tumori, Milano.

REFERENCES

1. Jemal A, Siegel R, A, Ward E, Murray T, Xu J, Thun MJ. Cancer statistics, 2007. *CA Cancer J Clin* 2007;57:43-66.
2. Ozols RF, Bookman MA, Connolly DC, et al. Focus on epithelial ovarian cancer. *Cancer Cell* 2004;5:19-24.
3. Balli S, Fey MF, Hanggi W, et al. Ovarian cancer. An institutional review of patterns of care, health insurance and prognosis. *Eur J Cancer* 2000;36:2061-8.

4. Negendank WG. Studies of human tumors by MRS: a review. *NMR Biomed* 1992;5:303-24.
5. de Certaines JD, Larsen VA, Podo F, Carpinelli G, Briot O, Henriksen O. In vivo ^{31}P MRS of experimental tumours. *NMR Biomed* 1993;6:345-65.
6. Podo F. Tumour phospholipid metabolism. Review article. *NMR Biomed* 1999;12:413-39.
7. Ackerstaff E, Glunde K, Bhujwalla ZW. Choline phospholipid metabolism: a target in cancer cells? *J Cell Biochem* 2003;90:525-33. Hara T. ^{18}F -Fluorocholine: a new oncologic PET tracer. *J Nucl Med* 2001;42:1815-17.
8. Hara T. ^{18}F -Fluorocholine: a new oncologic PET tracer. *J Nucl Med* 2001;42:1815-17.
9. Torizuka T, Kanno T, Futatsubashi M, et al. Imaging of gynecologic tumors: comparison of ^{11}C -choline PET with ^{18}F -FDG PET. *J Nucl Med* 2003;44:1051-56.
10. Aboagye EO, Bhujwalla ZM. Malignant transformation alters membrane choline phospholipid metabolism of human mammary epithelial cells. *Cancer Res* 1999;59:80-4.
11. Glunde K, Jie C, Bhujwalla M. Molecular causes of the aberrant choline phospholipid metabolism in breast cancer. *Cancer Res* 2004; 64:4270-76.
12. Kurhanewicz J, Vigneron DB, Nelson SJ. Three-dimensional magnetic resonance spectroscopic imaging of brain and prostate cancer. *Neoplasia* 2000;2:166-89.
13. Podo F, Sardanelli F, Iorio E, Canese R, Carpinelli G, Alfonso F and Canevari S. Abnormal Choline Phospholipid Metabolism in Breast and Ovary Cancer: Molecular Bases for Noninvasive Imaging Approaches. *Curr Med Imaging Rev* 2007;3,123-37.
14. Ferretti A, D'Ascenzo S, Knijn A, Iorio E., Dolo V, Podo F. Detection of polyol accumulation in a new ovarian carcinoma cell line, CABA 1: a ^1H NMR study. *Br J Cancer* 2002;86:1180-87.
15. Granata F, Iorio E, Carpinelli G, Giannini M, Podo F. Phosphocholine and phosphoethanolamine during chick embryo myogenesis: a ^{31}P -NMR study. *Biochim Biophys Acta* 2000;1483:334-42.
16. Iorio E, Mezzananza D, Alberti P, Spadaro F, Ramoni C, D'Ascenzo S, Millimaggi D, Pavan A, Dolo V, Canevari S, Podo F. Alterations of choline phospholipid metabolism in ovarian tumor progression. *Cancer Res* 2005;65:9369-9376.
17. Kaye S, Gershenson D, Hung M, Seiden M. Discussion: Molecular Therapeutics and Pharmacogenomics. *Gynecol Oncol* 2003; S93-S96.
18. Cook GJR. Oncological molecular imaging: nuclear medicine techniques. *Br J Radiol* 2003;76:S152-8.
19. Tian M, Zhang H, Higuchi T, Oriuchi N, Endo K. Oncological diagnosis using (^{11}C) -choline-positron emission tomography in comparison with 2-deoxy-2- $[(^{18}\text{F})]$ fluoro-D-glucose-positron emission tomography. *Mol Imaging Biol* 2004;6:172-9.
20. Katz-Brull R, Lavin PT, Lenkinski RE. Clinical utility of proton magnetic resonance spectroscopy in characterizing breast lesions. *J Natl Cancer Inst* 2002;94:1197-203.